Imaging of molecular probe activity with Born-normalized fluorescence optical projection tomography

Claudio Vinegoni,[1,*] Paolo Fumene Feruglio,[1,2] Virna Cortez-Retamozo,[1] Daniel Razansky,[3] Benjamin D. Medoff,[4,5] Vasilis Ntziachristos,[3] Andrea Sbarbati,[2] Mikael Pittet,[1] and Ralph Weissleder[1]

[1]*Center for Systems Biology, Massachusetts General Hospital, Harvard Medical School, 185 Cambridge Street, Boston, Massachusetts 02114, USA*

[2]*Department of Morphological and Biomedical Sciences, University of Verona, Strada Le Grazie 8, 37134 Verona, Italy*

[3]*Institute for Biological and Medical Imaging (IBMI), Technical University of Munich and Helmholtz Center Munich, Ingolstaedter Landstrasse 1, 85764 Neuherberg, Germany*

[4]*Center for Immunology and Inflammatory Diseases, Division of Rheumatology, Allergy, and Immunology, Massachusetts General Hospital, Harvard Medical School, 149 13th Street, Charlestown, Massachusetts 02129, USA*

[5]*Pulmonary and Critical Care Unit, Massachusetts General Hospital, Harvard Medical School, Boston, Massachusetts 02114, USA*

**Corresponding author: cvinegoni@mgh.harvard.edu*

Received December 22, 2009; revised February 5, 2010; accepted February 5, 2010; posted February 26, 2010 (Doc. ID 121886); published March 31, 2010

Optical projection tomography is a new *ex vivo* imaging technique that allows imaging of whole organs in three dimensions at high spatial resolutions. In this Letter we demonstrate its capability to tomographically visualize molecular activity in whole organs of mice. In particular, eosinophil activity in asthmatic lungs is resolved using a Born-normalized fluorescence optical projection tomography and employing a near-IR molecular probe. The possibility to achieve molecularly sensitive imaging contrast in optical projection tomography by means of targeted and activatable imaging reporter agents adds a new range of capabilities for investigating molecular signatures of pathophysiological processes and a wide variety of diseases and their development.

OCIS codes: 110.0110, 170.0170, 170.3880.

A number of new molecular imaging tools are being developed with the underlying goal of diagnosing early disease and monitoring novel therapies over time. Molecular imaging applications are useful for investigations of the cardiovascular system [1,2], cancer biology [3], or gene expression. Among the different molecular imaging modalities the optical ones at the micro-, meso-, and macro-levels [4–6] play a major role allowing for *in vivo* and *ex vivo* imaging while providing different extent of resolution and penetration depths. Optical projection tomography (OPT) [7] is a high-resolution three-dimensional imaging technique that is based on transillumination measurements of both transmitted and emitted light through optically cleared *ex vivo* samples. Fluorescent and nonfluorescent biological samples up to 15 mm thick can be reconstructed with resolutions of up to 5–10 μm in three dimensions. Images are taken over 360° and absorption maps can be obtained using a common Radon backprojection algorithm, while fluorescent maps can be computed using a Born-normalized approach [8,9]. At present, the technology has been used to resolve the tissue distribution of fluorescent proteins or other probes that emit in the visible light range. Herein we demonstrate that the OPT can be used for resolving targeted and activatable near-IR (NIR) fluorescent molecular beacons providing a new powerful imaging methodology for molecular sensing. Because the fixation process and the chemical treatment necessary for the optical clearing of the sample both induce high level of autofluorescence, newer NIR probes are required. In particular we tested whether the molecular imaging contrast OPT could detect enzyme activity mediated by eosinophils in mice with inflamed lungs. We chose this model owing to the primary role that eosinophils play in response to allergen exposure.

While tomographic reconstructions of the transmitted signal are obtained using the inverse Radon transform, fluorescence molecular probe distributions can be correctly obtained using a Born-normalized approach that takes into account for the spatially dependent component of the excitation signal [8]. The normalized Born intensity U_B is defined as the ratio of the emission (fluorescence) measurements with the corresponding excitation measurements, i.e., $U_B = U_{\mathrm{fl}}/U_{\mathrm{ex}}$. By using the correct Green's functions for both excitation and emission the forward model of our imaging problem can be further simplified discretizing the volume of interest. The tomographic set of Born-normalized measurements can then be written as $U_B = WA$, where W is the forward model ("weight") matrix, while A represents the volumetric distribution of the molecular contrast agent (fluorophore concentration). The latter can subsequently be found by inverting W or, in a simplified manner, by directly applying the Radon backprojection to the set of measurements U_B. Depending on the imaged sample and contrast agent used a multispectral approach could be implemented in order to remove any eventual autofluorescence contribution using a linear unmixing algorithm.

A detailed representation of the experimental setup is shown in Fig. 1. A white-light source is filtered with a narrow bandpass interference filter (Chroma) centered at 680 nm with a 5 nm FWHM bandwidth. Uniform illumination of the sample is obtained via the use of a diffuser and a combined lens. The sample under investigation is kept fixed in a cylindrical agarose holder immersed in a benzyl alcohol and benzyl benzoate (BABB) solution filling an NIR antireflective-coated imaging chamber and rotated along its vertical axis. A rotational stage controller (Newport, PR50) allows for 360° rotation with an absolute accuracy of 0.05°. Three manual controllers adjust the tilt of the vertical axis in its orthogonal plane. The presence of an automatic shutter allows the control of light exposition in order to prevent the photobleaching of the molecular contrast agent.

The imaging system collects both transmitted and fluorescence signals in the transillumination mode. The intrinsic transmitted signal is directly detected by a CCD camera (VersArray from Roper Scientific/Princeton Instruments, Trenton, N.J., 24 μm pixel size) with a 512×512 (after 2×2 binning) imaging array using a telecentric system. The fluorescence signal from a molecular imaging agent is filtered through a narrow bandpass interference filter centered at 710 ± 5 nm coupled with a 710 nm longpass filter (Andover Inc., Salem, N.H.) and detected by the same camera with a 1 s exposure time. Images are then taken over 360 projections with a 1° rotational angle along the vertical axis. Filters can be easily interchanged to switch between measurements of intrinsic and fluorescence signal. Labview is used for acquisition and visualization. Reconstructions are obtained using the NVIDIA common unified device architecture (CUDA) technology [10]. A separate personal computer (PC) hosts a CUDA-enabled Tesla C1060 consisting of 240 streaming processors each running at 1.3 GHz with 4 Gbytes of dedicated GDDR3 onboard memory and ultrafast memory access with 102 Gbytes/s bandwidth per graphic processing unit. Data between the two PCs are exchanged via an ethernet cable. The overall implementation is described in more detail in [10]. Fluorescence reconstructions were obtained through an absorption weighted inverse method using a Born-normalized transillumination approach [8]. Acquisition times were equal to 8 min, while reconstruction times varied from 4 s to 1 min, depending on the implemented algorithm [10].

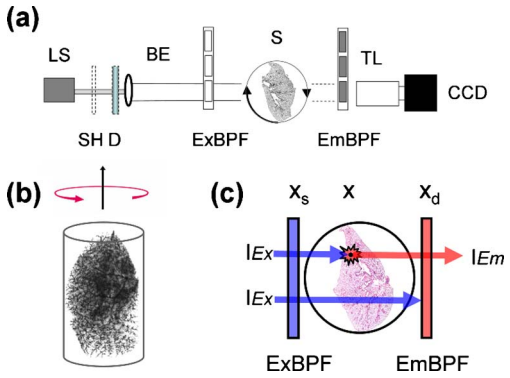

Fig. 1. (Color online) (a) Experimental setup: LS, light source; SH, shutter; D, diffuser; ExBPF, excitation wavelength filters; S, sample; EmBPF, fluorescence filters; TL, telecentric lens; CCD, imaging camera. (b) The imaged lung is held fixed in BABB solution embedded in an agarose gel cylinder. (c) After exciting the fluorophore located at position x, light at the emission wavelength λ_{fl} is filtered and collected by the CCD's pixel located at position x_d using a telecentric lensing system.

Female BALB/c mice were sensitized with chicken egg ovalbumin (OVA) protein in the presence of alum, followed by repeated challenge with the OVA alone. Monitoring the extent of eosinophil-mediated inflammation involved intravenous injection of an NIR metalloproteinase (MMP)-targeted sensor (MMPsense-680, Exc. 680 nm, Em. 710 nm), followed one day later by planar fluorescence diffusion imaging. The anesthesized mice were then prepared for the OPT imaging. To this end they received 50 μl of heparin intraperitoneally to avoid blood clotting, followed by longitudinal laparotomy, opening of the left renal vein, and infusion of 20 ml saline solution into the inferior vena cava. The lungs were collected after the blood was replaced with saline. Fluorescence reflectance imaging of the excised lungs revealed a strong MMP-targeted optical activity in mice challenged with the OVA [Fig. 2(b)]. No signal was detected in resting mice that received the MMP-agent [Fig. 2(e)]. Lungs were then fixed for 20 min in a 4% paraformaldehyde solution at 4°C, embedded in a 0.8% agarose gel, dehydrated through a series of 20%–100% ethanol solutions, and cleared by immersion in the BABB solution [7]. These steps were performed in the dark to prevent bleaching of the contrast agent and can be applied successfully independently of the specific targeted molecular agent or organ.

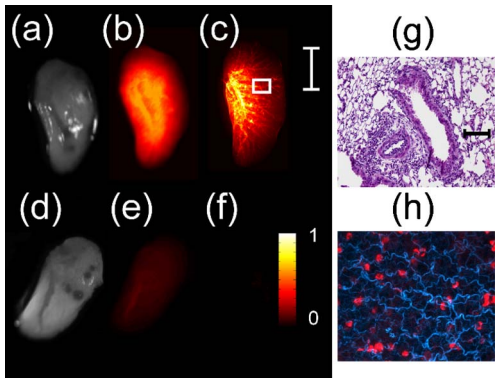

Fig. 2. (Color online) Eosinophil-mediated MMP activity in OVA-challenged mice in dissected and chemically cleared lungs. (a) White light and (b) fluorescence reflectivity image of explanted inflamed lungs injected with MMPsense. (c) Fluorescence transillumination image of cleared sample. (d)–(f) Corresponding images for a control mouse without MMPsense administration. The white bar corresponds to 5 mm. Color map scale in arbitrary units. (b) and (e) as well as (c) and (f) are normalized on the same scale. (g) Hemotoxylin and eosin staining of an inflamed lung section (20×; black bar corresponds to 0.1 mm). (h) Intravital microscopy image evidencing collagen structures and eosinophils. Location of (g) and (h) is marked by the white box in (c).

Lungs fluorescence transillumination imaging [Fig. 2(c)] detected strong fluorophore signal in the mice challenged with the OVA. Thus, the preparation of the tissue, including chemical treatment in the BABB solution, preserves fluorophore activity and is suitable for fluorescence optical tomographic imaging.

The OPT system is uniquely suited to resolve the distribution of molecular signal in three dimensions and in entire tissues. Born-normalized fluorescence OPT reconstructions of a lung lobe revealed that the MMP activity in OVA challenged mice localizes centrally and in the major bronchi (Fig. 3). Because the MMP activity is mostly found in eosinphils [11], the results likely illustrate the recruitment of eosinophils to the site of allergen deposition, i.e., in the lung mucosa and conducting airways. Accordingly, both histology [Fig. 2(g)] and *in vivo* microscopy [Fig. 2(h)] data confirmed the presence of inflammatory eosinophils at these locations. The OPT also revealed the spatial association of eosinophils to smaller bronchi and capillary vessels in the lungs, which was verified by histological analysis [Fig. 2(g)]. Thus, the OPT offers high-resolution imaging of the NIR molecular probe activity in different spatial orientations, and represents an attractive new tool for quantitative analysis of molecular information.

In conclusion, the present study demonstrates targeted molecular imaging contrast for the OPT and in particular shows the feasibility of visualizing eosinophil-associated MMP activity in mice with allergic airway inflammation. The approach can be used in combination with *in vivo* imaging techniques such as fluorescence molecular tomography [11]. The use of different probes specific to other biomarkers will extend the applications of the OPT and provide unprecedented combinatorial monitoring of different molecular events. NIR probes are particularly attractive in this context owing to low autofluorescence background present in a fixed tissue at those wavelengths. The implemented modality also offers the advantage to work in combination with both endogenously expressed fluorescent proteins and intrinsic absorption contrast as previously demonstrated by others [7], allowing one to obtain information from multiple targets.

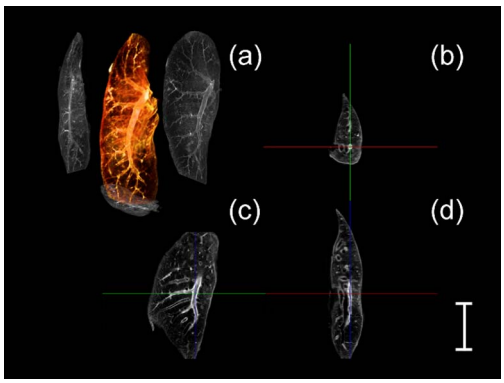

Fig. 3. (Color online) Normalized Born fluorescence reconstructions of an OVA-challenged mouse that received MMPsense 680. (a) Three-dimensional lung reconstruction; (b)–(d) coronal, axial, and saggital sections. The distribution of the molecular imaging contrast agent correlates well with the presence of eosinophils, the source of MMP activity, in lung parenchyma and conducting airways. White bar, 5 mm.

C. Vinegoni acknowledges support from the National Institutes of Health (NIH) grant 1-RO1-EB006432. We also acknowledge support from Veneto Nanotech and CARIVERONA Foundation.

References

1. F. A. Jaffer, D. E. Kim, L. Quinti, C. H. Tung, E. Aikawa, A. N. Pande, R. H. Kohler, G. P. Shi, P. Libby, and R. Weissleder, Circulation **115**, 2292 (2007).
2. F. Jaffer and R. Weissleder, Circ. Res. **94**, 433 (2004).
3. R. Weissleder and C.-H. Tung, Nat. Biotechnol. **17**, 375 (1999).
4. V. Ntziachristos, J. Ripoll, L. Wang, and R. Weissleder, Nat. Biotechnol. **23**, 313 (2005).
5. C. Vinegoni, C. Pitsouli, D. Razansky, N. Perrimon, and V. Ntziachristos, Nat. Methods **5**, 45 (2008).
6. D. Razansky, M. Distel, C. Vinegoni, R. Ma, N. Perrimon, R. Koester, and V. Ntziachristos, Nat. Photonics **3**, 412 (2009).
7. J. Sharpe, U. Ahlgren, P. Perry, B. Hill, A. Ross, J. Hecksher-Sorensen, R. Baldock, and D. Davidson, Science **296**, 541 (2002).
8. C. Vinegoni, D. Razansky, J. Figuereido, M. Nahrendorf, V. Ntziachristos, and R. Weissleder, Opt. Lett. **34**, 319 (2009).
9. C. Vinegoni, D. Razansky, J. L. Figueiredo, L. Fexon, M. Pivovarov, M. Nahrendorf, V. Ntziachristos, and R. Weissleder, JoVE 28, http://www.jove.com/index/details.stp?id=1389.
10. C. Vinegoni, L. Fexon, P. Fumene Feruglio, M. Pivovarov, J. L. Figueiredo, M. Nahrendorf, A. Pozzo, A. Sbarbati, and R. Weissleder, Opt. Express **17**, 22320 (2009).
11. V. Retamozo, F. K. Swirski, P. Waterman, H. Yuan, J. L. Figueiredo, A. P. Newton, R. Upadhyay, C. Vinegoni, R. Kohler, J. Blois, A. Smith, M. Nahrendorf, L. Josephson, R. Weissleder, and M. J. Pittet, J. Clin. Invest. **118**, 4058 (2008).